Nuclear Engineering and Technology 51 (2019) 731–737

Contents lists available at ScienceDirect

Nuclear Engineering and Technology

journal homepage: www.elsevier.com/locate/net

Original Article

A novel approach in voltage transient technique for the measurement of electron mobility and mobility-lifetime product in CdZnTe detectors

H. Yücel [a, *], Ö. Birgül [b], E. Uyar [a], Ş. Çubukçu [c]

[a] Ankara University, Institute of Nuclear Sciences, Tandoğan, 06100, Ankara, Turkey
[b] Ankara University, Faculty of Engineering, Dept. of Biomedical Engineering, Gölbaşı, Ankara, Turkey
[c] Ankara University, Faculty of Engineering, Dept. of Physics Engineering, Tandoğan, 06100, Ankara, Turkey

ARTICLE INFO

Article history:
Received 14 May 2018
Received in revised form
27 October 2018
Accepted 29 December 2018
Available online 31 December 2018

Keywords:
CdZnTe
Electron mobility
Mobility-lifetime product
Transient pulse
Rise time
Charge Carrier
Digital pulse processing

ABSTRACT

In this study, a new measurement method based on voltage transients in CdZnTe detectors response to low energy photon irradiations is applied to measure the electron mobility (μ_e) and electron mobility-lifetime product $(\mu\tau)_e$ in a CdZnTe detector.

In the proposed method, the pulse rise times are derived from low energy photon response to 59.5 keV(^{241}Am), 88 keV(^{109}Cd) and 122 keV(^{57}Co) γ-rays for the irradiation of the cathode surface at each detector for different bias voltages. The electron $(\mu\tau)_e$ product was then determined by measuring the variation in the photopeak amplitude as a function of bias voltage at a given photon energy using a pulse-height analyzer. The $(\mu\tau)_e$ values were found to be $(9.6 \pm 1.4)\times10^{-3}$cm^2 V^{-1} for 1000 mm^3, $(8.4 \pm 1.6)\times10^{-3}$cm^2 V^{-1} for 1687.5 mm^3 and $(7.6 \pm 1.1)\times10^{-3}$ cm^2 V^{-1} for 2250 mm^3 CdZnTe detectors. Those results were then compared with the literature $(\mu\tau)_e$ values for CdZnTe detectors.

The present results indicate that, the electron mobility μ_e and electron $(\mu\tau)_e$ values in CdZnTe detectors can be measured easily by applying voltage transients response to low energy photons, utilizing a fast signal acquisition and data reduction and evaluation.

1. Introduction

In recent years, CdZnTe (CZT) semiconductor detectors have been commonly used in several fields such as nuclear security and safeguards, health physics and medical diagnostics, environmental monitoring and other applications. This is due to their relatively good detection efficiency and reasonable energy resolution compared to other semiconductor detectors. CZT material is also suitable for operating at room temperatures as laboratory based X-ray/γ-ray spectroscopy devices because this material has a wide band-gap energy range of 1.53–1.64 eV. Other good properties of CZT such as good electron collection efficiency, room temperature polarization stability, long term stability and low leakage currents, which are due to their high bulk resistivity (10^{10}–10^{11} Ω cm) make present the important advantages as a detector material [1–3].

One of the fundamental figure-of-merits for a semiconductor X-ray/γ-ray detector is the transport properties of charge carriers [1]. The mobility (μ), lifetime (τ) and their product, (μτ) for electrons and holes are often used for the evaluation of its potential for various spectroscopy applications. For instance, the radiation detector materials having the highest μτ products provide the best energy resolution spectrometers [4]. However, CZT detector material suffers significantly from incomplete charge collection because it has much higher electron mobility (1350 $cm^2 \cdot V^{-1} \cdot s^{-1}$) than hole mobility (120 $cm^2 \cdot V^{-1} \cdot s^{-1}$), giving rise to relatively stationary hole movement within the electron collection time [5]. However, this poor charge collection due to hole trapping has been remarkably solved by developing a coplanar grid electrode(CPG) structure for CZT detectors, invented by Luke [6]. There are also other charge sensing methods such as parallel or capacitive Frisch-grids, steering grids, simple pixelated anodes to overcome the hole tailing in the peak by eliminating the effects of low hole mobility. The various electronic techniques are used for compensating for severe hole trapping such as pulse rise time compensation, pulse shape discrimination and charge-loss compensation techniques [7–9]. The advantages and limitations of single-polarity charge sensing methods were previously discussed in detail by He [10].

In order to determine the interaction depth of a particle in the detector, the pulse rise time method is also used for the characterization of the transport properties of the detector material. In

* Corresponding author.
E-mail address: haluk.yucel@ankara.edu.tr (H. Yücel).

https://doi.org/10.1016/j.net.2018.12.024

literature, different methods, for instance, rise time by α-particle response, time-of-flight (TOF), etc. were used for the measurement of mobility value. TOF charge drift mobility measurement is a direct method to reveal the transport properties of high-resistivity detector materials [11]. For this purpose, transient current signals from the sample were directly fed into a digital oscilloscope [12]. TOF method was employed to study the carrier transit time and mobility in CdZnTe and CdTe radiation detectors by using a pulsed laser that creates electron-hole pairs in the material [4].

A direct measurement technique based on single polarity charge sensing was used to improve the determination of $(\mu\tau)_e$ product [13]. In this technique, the value of $(\mu\tau)_e$ product was determined by using the variation in pulse heights at different bias voltages. The $(\mu\tau)_e$ product has recently been measured for pixelated CZT detectors by using data from a standard calibration measurement in which the electron mobility, the electron mean drift time and their product were compared against other method [19]. The drift mobility and the mobility-lifetime product of charge carriers in the pixelated CZT detector were also measured by using a transient pulse technique in which an ^{241}Am alpha source (5.48 MeV, alpha particle) and ^{133}Ba (81 keV, gamma photons) for the cathode irradiation was used as excitation source, respectively [14]. The electron drift-mobility and mobility-lifetime product measurements were also carried out on the CdZnTe planar geometry with Frisch collar and pixelated anode structures [15]. The electron drift-mobility was measured using a time-of-flight (TOF) method where the waveform of the response to alpha particles impinging on the cathode are recorded and averaged on a storage oscilloscope [16].

In this study, this time-of-flight method was modified for measurement of electron mobility for the case of the built-in CPG CdZnTe detector. In fact, there is no fundamental difference between the TOF method and voltage transient technique. However, the electron mobility was calculated from the rise time of the pulse instead of the transit time using the recorded pulse shapes for charge signals induced on the anode for the electron transport property. Normally, with a fast oscilloscope, one can measure the charge collection time in current mode or the voltage rise time, t_r, which is related to charge carrier drift velocity. So this modified TOF method is called here as voltage transient technique. The applied technique has some novelty to determine charge transport properties of a CZT material since it was employed on a real CZT gamma-ray spectrometer. That is, the CZT material was not investigated through an application-specific integrated circuit(ASIC). The voltage transient method consists of fully irradiating the surface of cathode side of the built-in CZT detector by a low energy photon source irradiation instead of either alpha particle or laser excitation. Thus, pulse heights were obtained to extract the induced charge on the electrode for charge carriers at the different bias voltage transients with the help of a fast digital oscilloscope.

For the measurement of the $(\mu\tau)_e$, ^{241}Am (59.6 keV) and ^{57}Co (122.06 keV) gamma-ray sources were also used as excitation source [17,18].

In general, the measurements on the $(\mu\tau)_e$ product is based on the Hecht relation and/or direct charge sensing methods for the coplanar grid CZT detectors [13]. The induced signal measured from CZT crystal will entirely be due to the movement of the electrons since the holes are virtually stationary during the electron drift [19]. Hence, the mobility-lifetime product $(\mu\tau)_e$ can be determined by measuring the photopeak shift as a function of applied bias.

In the present study, a direct measurement technique based on single polarity charge sensing was used to measure the electron $(\mu\tau)_e$ product. To apply this method, a complete pulse-height analyzer was set up in an analog chain of NIM modules and the variation in photopeak amplitudes was measured as a function of bias voltages applied to the CPG-CZT detector at a given photon energy. In our study, a low gamma energy 59.6 keV (^{241}Am) source was used for excitation to irradiate the full CZT cathode surface in the detector.

2. Experimental setup

Three coplanar grid CZT detectors with 1000 mm^3, 1687.5 mm^3 and 2250 mm^3 size (purchased from eV Products Inc.) were used in this study. Their main specifications such as energy resolution, crystal dimensions, and operating bias voltage are given in our previous work [20]. Two of the detectors have 10 mm crystal thickness and the other one has 7.5 mm thickness. The detector window is 0.35 mm thick aluminum. The spacing between the crystal and the window is specified as 1.91 mm nominal. The detector was shielded in annuli cylinders that are 1 cm thick stainless steel and 2 cm thick Pb with an inside lining of 1 mm Cu to reduce room background γ-rays and low energy K X-rays. In the measurements, a lead collimator having a height/diameter ratio of 2.4 was used to establish a “good” counting geometry condition. A collimator with a hole diameter of either 10 mm or 15 mm was used in each configuration so that the source nearly subtends the whole active crystal surface area. In the experimental configuration, the distance between the source and the detector was adjusted taking the solid angle into account so that the full cathode surface was irradiated with the photon source. The radioisotope sources, ^{22}Na, ^{57}Co, ^{54}Mn, ^{60}Co, ^{65}Zn, ^{109}Cd and ^{137}Cs purchased from Eckert&Ziegler Inc. and Czech Metrology Institute were used in the measurements. Each source has an active diameter of 3 mm and their capsules have 25.4 mm outer diameter and 3.18 mm thickness. However, ^{241}Am and ^{57}Co sources were encapsulated within EG1 and EG3X capsules having a 25 mm outer diameter and 3 mm thickness.

The detector is connected to its built-in front-end electronics consisting of two charge-sensitive preamplifiers and a differential amplifier in its housing. The setups shown in Fig. 1 were used to measure both the electron mobility and mobility-life time product of the CZT crystals. In setup 1 shown in Fig. 1, the preamplifier signals were sent to the pulse shaping amplifier and then to a Multiport II MCA unit (Canberra Inc.) to acquire the spectral response of a gamma-ray source. The gamma acquisition was performed through Genie 2000™ software.

The pre-amplified signals from both anode and cathode (marked as A and B in setup 2) were directly fed to a difference amplifier (B-A) and the resulting signals due to electrons-only were captured by using a fast digital oscilloscope (LeCroy Wave Runner Model 62xi, frequency: 600 MHz, maximum sampling rate: 10 GS/s).

The voltage transient pulses were captured by the digital oscilloscope that was adjusted to a trigger level of −80 mV, vertical axis of 500 mV/division and time base of 200 μs/division. The pulse sampling rate was chosen as 100 MS/s and each signal was automatically captured and saved in MATLAB™ data format. These signals were then evaluated to derive the rise time information from each captured signal by employing MATLAB™.

For gamma spectrum acquisition, a gamma-ray spectrometer consisting of a spectroscopy amplifier (Canberra 2025), a fixed conversion time and 16 K channels ADC/MCA (Canberra Multiport-II) and a power supply (Canberra 3106 D) was used with the coplanar grid CZT detector. Lower level discriminator (LLD) was set to 12 channels in ADC to exclude the soft x-rays, including the average electronic noise level of ~10.5 keV (corresponding to 9 channels width) in the acquired γ-ray spectra.

For pulse height analysis, the signals were processed with a shaping time of 1 μs and digitized into 2048 channels MCA

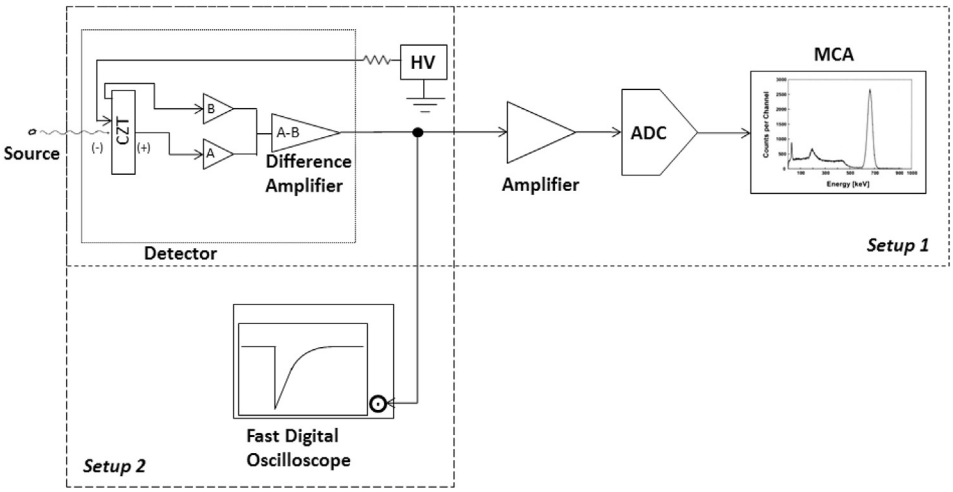

Fig. 1. Measurement configurations for a CdZnTe detector.

memory. The photopeak centroids were determined from the acquired gamma-ray spectra, where the acquisition period (live time) was chosen to accumulate at least 50000 counts in the peak of interest. This depends on the used source activity at a given geometry. The background spectrum was subtracted from each source spectrum by stripping on a channel-by-channel basis.

3. Results and discussion

In the present study, photon irradiations with low energy were performed on the full cathode surface to measure electron mobility by using pulse rise time method and the electron mobility life time by using pulse height analysis method as follows.

3.1. Measurement of the electron mobility, μ_e

For the measurement of electron mobility the pulses from the detector preamplifier output were recorded at a sampling rate of 100 MS/s for the bombardment of the low photon energies of 59.6 keV (^{241}Am), 88 keV (^{109}Cd) and 122 keV (^{57}Co). The voltage transient pulses were obtained for each -detector combination and the applied high voltage was changed in the range from −600 V to −1400 V depending on detectors' maximum bias voltage.

A typical pulse recorded is shown in the insert of Fig. 2. MATLAB™ was used to evaluate and display the results. The transition region of pulses for five different bias voltages for 1000 mm^3 detector for the case of ^{241}Am source excitation are also plotted. In order to be able to compare transition behavior of different pulses, amplitudes were normalized to their own peak value. Pulses with average rise time value were chosen. A five point weighted moving average smoothing filter with weights [1 3 5 3 1] was used on the pulses.

Firstly, the peak values of all pulses were found and a histogram of these peak values was investigated to eliminate any spurious recordings. Mean peak value ($V_{p,mean}$) and its standard deviation ($V_{p,std}$) were calculated and pulses with peak value inside the range from ($V_{p,\ mean}$ - $V_{p,\ std}$) to ($V_{p,\ mean}$ + $V_{p,\ std}$) were used for evaluations. Out of 7640 pulses recorded in MATLAB™ data format, 5415 pulses met this criterion and were included in rise time calculations. As shown as an example in Fig. 2, the pulse rise time of a digital signal was evaluated by taking into account of both 10-90% and 10-95% of the signal amplitude.

For the irradiation of 59.6 keV, 88 keV and 122.1 keV photons, mean pulse rise times obtained from the transient pulses at

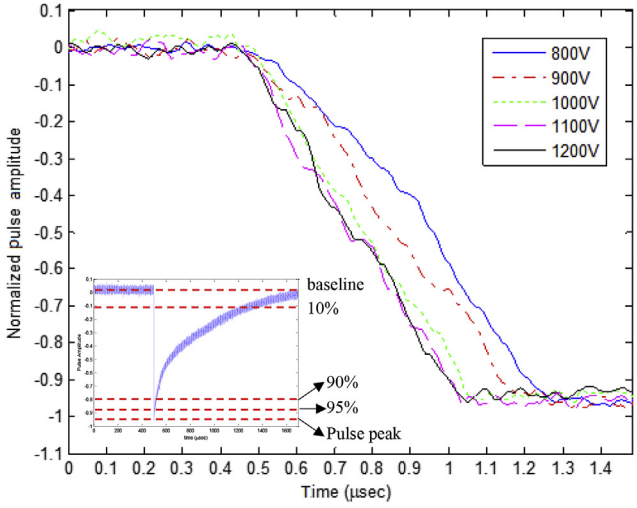

Fig. 2. A comparison of high-voltage transients used in determination of electron mobility.

different bias voltages are given in Table 1 together with their standard deviations.

The electron mobility for a CZT detector is deduced from the mean drift velocity versus the electric field applied to the crystal as follows:

$$\mu_e = \frac{D^2}{V \cdot t_r} \tag{1}$$

where D is the thickness of the crystal, t_r is the charge carrier (electron) rise time (less than the transit time) and V is the applied high voltage.

For the ideal case when no carrier trapping occurs, the drift of electrons across the crystal produces a constant current (thus induced charge at the electrode) whose duration is the transit time t_r of electrons. In this evaluation, it is assumed that a uniform electric field distribution is established in the whole crystal. The weighted mean rise times are used to calculate the mean electron drift velocity at each photon energy. Then the drift velocities (in cm/s) are plotted against the increasing electric field (in V/cm).

An example is shown in Fig. 3 for three CZT detectors when irradiated with 59.6 keV energy photons. This plot shows a linear

Table 1
Measured pulse rise times for the transient pulses at different bias voltages applied to CZT detectors.

CdZnTe Detector	Bias Voltage	^{241}Am (59.6 keV)		^{109}Cd (88.03 keV)		^{57}Co (122.06 keV)	
		Mean pulse rise time[a]		Mean pulse rise time[a]		Mean pulse rise time[a]	
	V_b (Volt)	10–90% t_r (μs)	10–95% t_r (μs)	10–90% t_r (μs)	10–95% t_r (μs)	10–90% t_r (μs)	10–95% t_r (μs)
Detector 1 (10x10 × 10 mm^3)	800	0.58 ± 0.26	0.64 ± 0.28	0.60 ± 0.29	0.69 ± 0.35	0.64 ± 0.25	0.76 ± 0.34
	900	0.56 ± 0.2	0.63 ± 0.23	0.54 ± 0.26	0.61 ± 0.28	0.57 ± 0.25	0.63 ± 0.27
	1000	0.51 ± 0.20	0.57 ± 0.21	0.50 ± 0.21	0.57 ± 0.25	0.51 ± 0.19	0.60 ± 0.25
	1100	0.46 ± 0.18	0.54 ± 0.21	0.46 ± 0.18	0.52 ± 0.21	0.49 ± 0.18	0.54 ± 0.19
	1200	0.42 ± 0.16	0.49 ± 0.19	0.42 ± 0.15	0.47 ± 0.18	0.45 ± 0.16	0.50 ± 0.19
Detector 2 (15x15 × 7.5 mm^3)	600	0.69 ± 0.19	0.86 ± 0.31	0.69 ± 0.17	0.79 ± 0.22	0.64 ± 0.22	0.83 ± 0.32
	700	0.57 ± 0.17	0.66 ± 0.19	0.58 ± 0.15	0.68 ± 0.21	0.59 ± 0.14	0.68 ± 0.17
	800	0.53 ± 0.13	0.61 ± 0.17	0.51 ± 0.14	0.58 ± 0.16	0.50 ± 0.14	0.61 ± 0.22
	900	0.44 ± 0.12	0.52 ± 0.17	0.47 ± 0.11	0.58 ± 0.21	0.45 ± 0.12	0.53 ± 0.20
	1000	0.41 ± 0.09	0.46 ± 0.11	0.39 ± 0.11	0.48 ± 0.18	0.41 ± 0.10	0.48 ± 0.13
Detector 3 (15x15 × 10 mm^3)	1000	0.62 ± 0.23	0.69 ± 0.26	0.63 ± 0.21	0.72 ± 0.27	0.63 ± 0.23	0.72 ± 0.26
	1100	0.56 ± 0.19	0.66 ± 0.26	0.58 ± 0.21	0.65 ± 0.22	0.56 ± 0.21	0.62 ± 0.21
	1200	0.52 ± 0.17	0.58 ± 0.18	0.54 ± 0.17	0.60 ± 0.19	0.52 ± 0.18	0.58 ± 0.20
	1300	0.46 ± 0.16	0.55 ± 0.25	0.49 ± 0.16	0.56 ± 0.22	0.49 ± 0.15	0.55 ± 0.18
	1400	0.42 ± 0.15	0.48 ± 0.18	0.48 ± 0.14	0.53 ± 0.17	0.44 ± 0.14	0.52 ± 0.17

[b)]Weighted averages were obtained from the arithmetic mean values of rise times that are estimated by taking into 10-90% and 10-95% of the pulse amplitude.
[a] Mean values were obtained from the rise time values of about 200 pulses sampled at 100 MS/s in a digitized wave form at every bias voltage. The uncertainty is estimated by taking standard deviation of about 200 pulses, which were captured at every bias voltage for each detector.

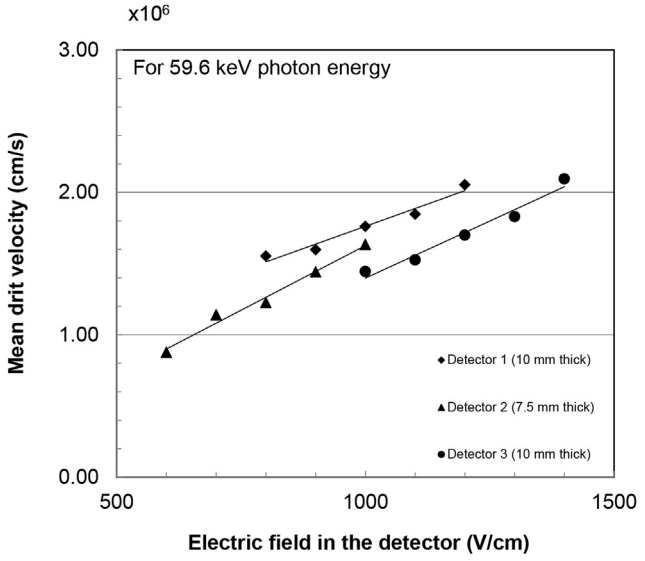

Fig. 3. Mean drift velocity versus applied electric field in CdZnTe detectors for 59.6 keV photon energy.

relation between the electric field and the mean drift velocity. When the measured data are fitted to a linear function, the slopes give us the electron mobility in a CZT detector. The results for electron mobility, μ_e, for three different detectors are given in Table 3 from the linear regression analysis.

The overall combined uncertainty in the mobility values ranged from 5.6 to 30.4% within ±1σ limits. The results for the mobility of 10 mm thick CZT crystals in Table 2 was found to be 1236 ± 153 and 1557 ± 170 $cm^2 \cdot V^{-1} \cdot s^{-1}$ when irradiated with 59.6 keV photons, thus resulting in a weighted value μ_e of 1379 ± 114 $cm^2 \cdot V^{-1} \cdot s^{-1}$ is estimated for CZT detectors. The μ_e value for a 10 mm thick CZT crystals (eV Products Inc.) agrees with that of 1350 $cm^2 \cdot V^{-1} \cdot s^{-1}$ given by Knoll by ~2.1%.

Table 3
Measured results for the electron $(\mu\tau)_e$ mobility-lifetime product for three coplanar grid CdZnTe detectors using low γ-ray energies.

Detector number (Crystal size)	Electron mobility-lifetime product $(\mu\tau)_e$ (10^{-3} $cm^2 \cdot V^{-1}$)[a]	
	Using 59.6 keV γ-ray	Using 88 keV γ-ray
Detector 1 (10x10 × 10 mm^3)	9.6 ± 1.4	12.1 ± 1.7
Detector 2 (15x15 × 7.5 mm^3)	8.4 ± 1.9	12.3 ± 3.1
Detector 3 (15x15 × 10 mm^3)	7.6 ± 1.1	11.1 ± 1.6

[a] The overall combined uncertainty is given within ±1σ limits (at a 68.4% confidence level).

3.2. Measurement of the electron mobility-lifetime product, $(\mu\tau)_e$

In determining the electron mobility-lifetime product $(\mu\tau)_e$ of the used CZT detectors were exposed to both low and high energy γ-ray sources on the cathode side such that the electron cloud created due to photon interactions would be drifted over the entire detector thickness. The mobility-life time product, $(\mu\tau)_e$, of charge carriers are traditionally determined by the Hecht's equation. However, an alternative technique for measuring $(\mu\tau)_e$ can be employed based on the photopeak centroid shift at two bias voltages using the direct charge sensing method, as suggested by He et al.[13]

Table 2
Measured results for the electron mobility, μ_e using low γ-ray energies for three coplanar grid CZT detectors.

Detector number (Crystal size)	Electron mobility μ_e ($cm^2 \cdot V^{-1} \cdot s^{-1}$)[a]		
	59.6 keV (^{241}Am)	88 keV (^{109}Cd)	122.1 keV (^{57}Co)
Detector 1 (10x10 × 10 mm^3)	1236 ± 153	1638 ± 93	1640 ± 144
Detector 2 (15x15 × 7.5 mm^3)	1367 ± 110	1101 ± 136	1208 ± 48
Detector 3 (15x15 × 10 mm^3)	1557 ± 170	1205 ± 58	1335 ± 128

[a] The overall combined uncertainty is given within ±1σ limits (at a 68.4% confidence level).

In this measurement technique, the pulse heights can easily be measured from the observed peak centroid positions, H_1 and H_2, in channels from events originating near the cathode side at two different applied voltages, V_1 and V_2. The measured pulse heights are proportional to the induced charge (i.e., number of electrons) collected at the anode surface. Thus the electron $(\mu\tau)_e$, product is simply calculated by the following equation [17,21]

$$(\mu\tau)_e = \frac{D^2}{\ln(H_1/H_2)} \cdot \left(\frac{1}{V_2} - \frac{1}{V_1}\right) \quad (2)$$

where D is the detector crystal thickness (cm). At least 20000 counts, but in general, 50000 counts were accumulated in each photopeak of interest in the acquired γ-ray spectra and then the photopeak centroid positions were measured at two different applied (bias) voltages.

It was previously noted that this technique can be applied for either α-sources or low energy γ-rays, and if radiation is incident from the cathode surface no depth sensing is necessary [13]. Hence, low energy γ-ray sources (e.g. 59.6 keV (^{241}Am) and 88 keV (^{109}Cd)) were used in the measurements. Photons with these energies would interact near the cathode surface in the crystal, and therefore are suitable for the measurement of the induced electron charge. As an example, the mobility-lifetime product $(\mu\tau)_e$ results for 15x15 × 10 mm^3 CZT detector using 59.6 keV γ-ray are shown in Fig. 4.

The uncertainty in the measurement of the electron mobility-lifetime product $(\mu\tau)_e$ can be estimated by applying normal error propagation law to Eq. (2). It can be assumed that the photopeak has a Gaussian distribution with an expected value of H, which is the centroid of the photopeak. Its standard deviation is estimated from the pulse height spectrum as $\sigma(H) = FWHM/(2.355 \times \sqrt{N})$, where FWHM(%) is typical measured energy resolution [20] and N is the total number of γ-ray events contributing to the photopeak.

As an example, the peak area was 50000 counts for a 10x10 × 10 mm^3 CZT detector, and it was estimated that electron transport loss fraction was between 1% (i.e., $H_1/H_2 = 0.99$) and 2.5% (i.e., $H_1/H_2 = 0.975$). Additionally, FWHM value was measured to be 22.6% at 59.6 keV from the spectrum. Then the corresponding relative standard deviation of $(\mu\tau)_e$ value was calculated as:

$$\frac{\sigma(\mu\tau)_e}{(\mu\tau)_e} \approx \frac{1}{\ln(0.99)} \cdot \frac{22.6\%}{2.355 \cdot \sqrt{50000}} \cdot \sqrt{2} \approx 6.04\%$$

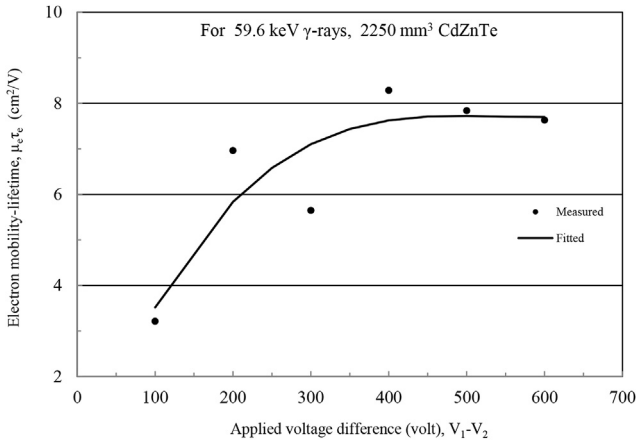

Fig. 4. Measured electron $(\mu\tau)_e$-product values with 59.6 keV γ-rays for a 2250 mm^3 coplanar grid CdZnTe detector. The $(\mu\tau)_e$ values for three different CZT detectors using 59.6 keV (^{241}Am) and 88 keV (^{109}Cd) γ-rays are given in Table 3.

The resulting uncertainties in Eq. (2) were estimated to be 2.40–6.04% at the peak centroids. The other uncertainty sources are mainly due to ADC/MCA nonlinearity (±0.025%), the amplifier integral nonlinearity (±0.04%) and the output stability of the power supply unit of ≤0.02% per 8 h period at normal operating conditions as specified in manufacturer manuals. Since crystal thickness tolerance is not quoted in the specification sheets of the present CZT materials by its manufacturer, D is assumed to be its final size with no uncertainty. Assuming additional type B uncertainties is about 5%, the overall measured uncertainties in $(\mu\tau)_e$ derived by Eq. (2) were estimated conservatively between 5.55% and 7.85%.

For comparison, the $(\mu\tau)_e$ values in the literature for single charge sensing CZT devices are given in Table 4, together with the measured $(\mu\tau)_e$ values in this study. For instance, high electron mobility-lifetime product (3.3×10^{-3} to 6×10^{-3} cm^2 V^{-1}) for three single crystal detector volumes of 10x10 × 7.5 mm^3 CZT detectors originally fabricated as coplanar-grid devices, however, the presence of non-uniform charge collection regions in the detectors are believed to cause the loss of spectroscopic performance [25] When the results for two detectors with similar crystal sizes (15x15 × 10 mm^3 CZT of He et al. [13] and 15x15 × 9.5 mm^3 CZT of Sturm et al. [21] are compared, it is seen that $(\mu\tau)_e$ values are between 4.1-10.1 × 10^{-3} cm^2 V^{-1} whereas the $(\mu\tau)_e$ value obtained for 15x15 × 10 mm^3 CZT detector used in this study is measured to be 7.6 ± 1.1 × 10^{-3} cm^2 V^{-1}. Similarly, for 10x10 × 10 mm^3 detector, $(\mu\tau)_e$ values reported in Table 4 vary between 6.9 × 10^{-3} cm^2 V^{-1} and 7.7 × 10^{-3} cm^2 V^{-1} where for the same size detector, it is found to be (9.6 ± 1.4) × 10^{-3} cm^2 V^{-1} in the present study. The differences may be attributed to the differences in detector material quality due to defects, impurities and manufacturing process. When a coplanar grid CZT detector is used as γ-ray spectrometer, it is clearly seen that spectroscopic performance is closely related to $(\mu\tau)_e$ value, which depends mainly on its intrinsic material quality.

It is also a fact that the higher energy γ-rays can penetrate inside the bulk of CZT semiconductor materials, so they cannot give the correct measure of the electron $(\mu\tau)_e$ product. Nevertheless, additional measurements were carried out for testing the electron $(\mu\tau)_e$ product behavior with increasing γ-ray energies. As shown in Fig. 5, the electron $(\mu\tau)_e$ product values for a 1000 mm^3 CdZnTe are saturated at about 122.1 keV (^{57}Co) γ-ray energy. These results indicate that photon with low energies such as 59.6 keV should be used to obtain photon a interactions below the contact surface.

As expected, the energy dependence of the electron $(\mu\tau)_e$ product values exhibited almost the same saturation behavior for all three detectors. This implies that the higher energy events occurred in deeper positions in the CZT crystal, thus the electrons spent shorter drifting time arriving at anode electrode and also the mean free drift length of an electron is shorter.

Although an alpha-particle spectrum has a single sharp peak (5.48 MeV) with little background to obtain a uniform electron transport in CZT crystal, the photon irradiation with low energies such as 59.6 keV (^{241}Am) can also provide sufficient electron charge over the cathode surface of a CZT crystal and this can be swept by uniform electric field. Thus, the electron mobility and mobility-life time product can be simply determined as described above. However, as the alpha particle range is ~0.025 mm in Al for 5.5 MeV energy [26], the 5.5 MeV alpha particles cannot penetrate through the 0.35 mm thick Al window of the present detector. Therefore, this alpha particle response technique is not practical for the case of a coplanar-grid CZT crystal built-in a detector housing. In the present study, photon irradiations with low energy of 59.6 keV were performed on the full cathode surface to measure electron mobility as a new approach. It creates electron-hole pairs almost below the crystal surface because of its very short penetration depth of ~0.32 mm, based its density of 5.8 g·cm^{-3} and mass attenuation

Table 4
Comparison of the electron $(\mu\tau)_e$ product values for CdZnTe detectors based on single charge sensing.

Detector size (Detector type[a], ID)	*Electron mobility-lifetime product*, $(\mu\tau)_e$		
	Measured value, $\mu_e\tau_e$ (10^{-3} $cm^2 \cdot V^{-1}$)	Measurement Method	Reference
10x10 × 10 mm^3 (coplanar grid, 06-10071)	9.6 ± 1.4	Direct single charge sensing	Present work
15x15 × 7.5 mm^3 (coplanar grid, 10-100-48)	8.4 ± 1.9	Direct single charge sensing	Present work
15x15 × 10 mm^3 (coplanar grid, 12-10074)	7.6 ± 1.1	Direct single charge sensing	Present work
19.5 × 19.5 × 5 mm^3 (pixelated detector)	6.2[c]	Charge collection efficiency using alpha spectroscopy	[16]
11.1 × 11.1 × 10 mm^3 (Frisch collar detector)	2.7[c]	Charge collection efficiency using alpha spectroscopy	[15]
5.9 x5.9 × 5 mm^3 (pixelated detector)	9.88 ± 2.33	Transient pulse technique	[14]
20x20 × 15 mm^3 (pixelated detector, No.1)	12.7 ± 1.7	Modified single charge sensing	[19]
20x20 × 15 mm^3 (pixelated detector, No.1)	14.1 ± 8.4	Direct single charge sensing	[19]
20x20 × 15 mm^3 (pixelated detector, No.2)	10.1 ± 0.9	Modified single charge sensing	[19]
20x20 × 15 mm^3 (pixelated detector, No.2)	10.6 ± 3.0	Direct single charge sensing	[19]
10x20 × 20 mm^3 (pixelated detector, No.2)	21[c]	Direct single charge sensing	[22]
5x5x0.9 mm^3 (Multiple electrode)	1.1[c]	No method specified	[1] [23]
15x15 × 9.5 mm^3 (coplanar grid)	7.92–10.12	Direct single charge sensing	[21]
10x10 × 10 mm^3 (coplanar grid,704474)	7.7[b]	Direct single charge sensing	[13]
15x15 × 5 mm^3 (coplanar grid, L1643#1)	7.2[b]	Direct single charge sensing	He et al. [13]
15x15 × 10 mm^3 (coplanar grid, 700033)	4.1[b]	Direct single charge sensing	[13]
10x10 × 10 mm^3 (coplanar grid, 1315-04)	6.9[b]	Direct single charge sensing	[13]
4.2x6.2 × 6.5 mm^3 (Frisch grid)	2.8[c]	Charge collection efficiency	[24]

[a] For this comparison, only single charge (electron) sensing CdZnTe devices are chosen.
[b] Typical uncertainty is specified as 5%.
[c] No uncertainty quote.

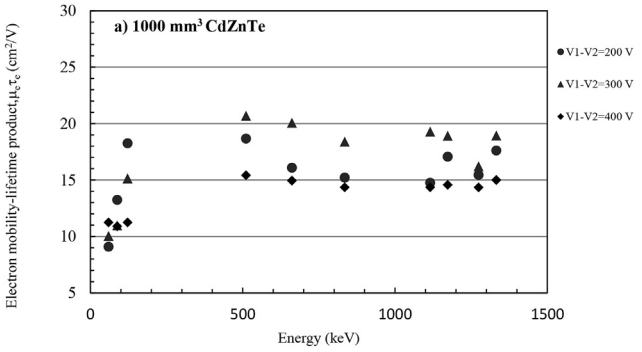

Fig. 5. Variation of the electron $(\mu\tau)_e$-product values with increasing γ-ray energies of 59.6–1274.5 keV for a 1000 mm^3 coplanar grid CdZnTe detectors.

coefficient of 5.299 $cm^2 \cdot g^{-1}$ [27]. This means that electron-hole pairs are created outside the active region of the detector and these electron hole pairs can have diffuse to the active region first where the electron mobility due to diffusion is slow compared to the electron mobility due to drift.

4. Conclusions

CZT semiconductor material can be considered as a practical and efficient radiation spectroscopy device if the detector material has appropriate charge transport quality properties. It is reported that, recent improvements in single crystal growth have largely eliminated the macroscopic defects but the microscopic defects such as possible Te-inclusions and precipitates in the crystals limit the spectroscopic performance of a CZT detector .[23] In determining the material quality and overall detector performance, the electron mobility, mean free drift time, and the $(\mu\tau)_e$ product are commonly measured quantities for studying semiconductor properties. These parameters are important especially to choose the detector grade materials and measurement of their performance when they used in x-ray/γ-ray spectroscopy.

In this study, the mobility and mobility-lifetime product were investigated in three large-volume coplanar grid CZT detectors. For low energy photon irradiation (59.6 keV) in the gamma ray CZT detector, the electron mobility was determined using voltage transient technique. From the deduced pulse rise time data, the electron mobilities were found to be in the range of 1236 ± 153 to 1557 ± 170 $cm^2 \cdot V^{-1} \cdot s^{-1}$ The weighted mean value was calculated to be 1373 ± 79 $cm^2 \cdot V^{-1} \cdot s^{-1}$ for 7.5–10 mm thick CZT crystals from eV Products Inc. and this value agrees with that of 1350 $cm^2 \cdot V^{-1} \cdot s^{-1}$ for CZT material given in Knoll's book (2000) by ~1.7% on average, even though it strongly depends on the material quality. Electron $(\mu\tau)_e$ products were measured to be (7.6 ± 1.1–9.6 ± 1.4) × 10^{-3} $cm^2 \cdot V^{-1}$ and these values agree with that of He et al. [13] and Sturm et al. [21] by 1.1%–19.5%.

Based on our results and comparisons with the literature, measurements using low energy gamma irradiation and voltage transient technique can be used to determine the electron transport properties of a CZT detector instead of alpha particle irradiation of a CZT material with time of flight method.

The present study indicate that, the electron mobility (μ_e) and electron $(\mu\tau)_e$ values in CdZnTe detectors can measured easily by applying voltage transients response to low energy photons. This can be accomplished by utilizing a fast signal acquisition, and making pulse data reduction and evaluation using a MATLAB™ tool.

Conflicts of interest

All authors have no conflicts of interest to declare.

Acknowledgements

This work was supported by The Scientific and Technological Research Council of Turkey (TÜBITAK) Research Grant No. 115S108. Authors are thankful to Dr. Ayşe Nur Esen who was assisted on some measurements.

Appendix A. Supplementary data

Supplementary data to this article can be found online at https://doi.org/10.1016/j.net.2018.12.024.

References

[1] M. Amman, J.S. Lee, P.N. Luke, H. Chen, S.A. Awadalla, R. Redden, G. Bindley,

Evaluation of THM-grown CdZnTe material for large-volume gamma-ray detector applications, IEEE Trans. Nucl. Sci. 56 (3) (2009) 795–799, 5076033.
[2] Z. He, G.F. Knoll, D.K. Wehe, J. Miyamoto, Position-sensitive single Carrier CdZnTe detectors, Nucl. Instrum. Methods Phys. Res. A. 338 (1–2) (1997) 180–185.
[3] T.E. Schlesinger, R.B. James, Semiconductors and Semimetals, vol. 43, Academic Press, San Diego, 1995, p. 339.
[4] J.C. Erickson, H.W. Yao, R.B. James, H. Hermon, M. Greaves, Time of flight experimental studies of CdZnTe radiation detectors, J. Electron. Mater. 29 (6) (2000) 699–703, https://doi.org/10.1007/s11664-000-0208-z.
[5] G.F. Knoll, Radiation Detection and Measurement, third ed., John Wiley & Sons, New York, 2000, p. 486.
[6] P.N. Luke, Single-polarity charge sensing in ionization detectors using coplanar electrodes, Appl. Phys. Lett. 65 (22) (1994) 2884–2886.
[7] J.E. Baciak, Nuclear Engineering and Radiological Sciences, Ph. D. thesis, University of Michigan, 2004.
[8] D.S. McGregor, in: C. Grupen, I. Buvat (Eds.), Handbook of Particle Detection and Imaging, Springer-Verlag, 2012, p. 384.
[9] B.W. Sturm, Nuclear Engineering and Radiological Sciences, Ph. D. thesis, University of Michigan, 2007.
[10] Z. He, Review of the Shockley-Ramo theorem and its application in semiconductor gamma-ray detectors, Nucl. Instrum. M*ethods Phys. Res*. A. 463 (1–2) (2001) 250–267.
[11] K. Suzuki, A. Iwata, S. Seto, T. Sawada, K. Imai, Drift mobility measurements on undoped $Cd_{0.9}$ $Zn_{0.1}$Te grown by high-pressure Bridgman technique, J. Cryst. Growth 214/215 (2000a) 909–912.
[12] K. Suzuki, S. Seto, A. Iwata, M. Bingo, T. Sawada, K. Imai, Transport properties of undoped $Cd_{0.9}$ $Zn_{0.1}$Te grown by high pressure bridgman technique, J. Electron. Mater. 29 (6) (2000b) 704–707.
[13] Z. He, G.F. Knoll, D.K. Wehe, Direct measurement of product of the electron mobility and mean free drift time of CdZnTe semiconductors using position sensitive single polarity charge sensing detectors, J. Appl. Phys. 84 (10) (1998) 5566–5569.
[14] H.Y. Cho, J.H. Lee, Y.K. Kwon, J.Y. Moon, C.S. Lee, Measurement of the drift mobilities and the mobility-lifetime products of charge carriers in a CdZnTe crystal by using a transient pulse technique, J. Inst. Met. 6 (2011) 1–7. C01025.
[15] S.K. Chaudhuri, Ramesh M. Krishna, Kelvin J. Zavalla, Liviu Matei, Vladimir Buliga, Michael Groza, Arnold Burger, Krishna C. Mandal, $Cd_{0.9}Zn_{0.1}$Te crystal growth and fabrication of large volume single-polarity charge sensing gamma detectors, IEEE Trans. Nucl. Sci. 60 (2013) 2853–2858.
[16] S.K. Chaudhuri, Khai Nguyen, Rahmi O. Pak, L. Matei, V. Buliga, M. Groza, A. Burger, K.C. Mandal, Large area $Cd_{0.9}Zn_{0.1}$Te pixelated detector: fabrication and characterization, IEEE Trans. Nucl. Sci. 61 (2014) 793–798.
[17] S.A. Awadalla, M. Al-Grafi, K. Iniewski, High voltage optimization in CdZnTe detectors, Nucl. Instrum. Methods Phys. Res. A. 764 (2014) 193–197.
[18] F. Zhang, Z. He, 3D position sensitive CdZnTe gamma-ray spectrometers - improved performance with new ASICs, Proc. SPIE, - Intl. Soc. Optic. Eng. 5540 (16) (2004) 135–143.
[19] Y.A. Boucher, F. Zhang, W. Kaye, Z. He, New measurement technique for the product of the electron mobility and mean free drift time for pixelated semiconductor detectors, Nucl. Instrum. Methods Phys. Res. A. 671 (2012) 1–5.
[20] H. Yücel, E. Uyar, A.N. Esen, Measurements on the spectroscopic performance of CdZnTe coplanar grid detectors, Appl. Radiat. Isot. 70 (8) (2012) 1608–1615.
[21] B.W. Sturm, Z. He, H. Zurbuchen, P.L. Koehn, Investigation of the asymmetric characteristics and temperature effects of CdZnTe detectors, IEEE Trans. Nucl. Sci. 52 (2068) (2005) 2068–2075, 2005). 52(5 III).
[22] Q. Li, A. Garson, P. Dowkontt, J. Martin, M. Beilicke, I. Jung, M. Groza, A. Burger, G. De Geronimo, H. Krawczynski, in: Proc. Of IEEE Nuclear Science Symposium (NSS'08), Dresden, Germany, 2008, 2008, pp. 484–489.
[23] L. Abbene, S. Del Sordo, F. Fauci, G. Gerardi, A. La Manna, G. Raso, A. Cola, E. Perillo, A. Raulo, V. Gostilo, S. Stumbo, Spectroscopic response of a CdZnTe multiple electrode detector, Nucl. Instrum. Methods Phys. Res. A. 583 (2–3) (2007) 324–331.
[24] R.M. Krishna, S.K. Chaudhuri, K.J. Zavalla, K.C. Mandal, Characterization of Cd0.9Zn0.1Te based virtual Frisch grid detectors for high energy gamma ray detection, Nucl. Instrum. Methods Phys. Res. A. 701 (2013) 208–213.
[25] S.A. Soldner, A.J. Narvett, D.E. Covalt, C. Szeles, Characterization of the charge transport uniformity of CdZnTe crystals for large-volume nuclear detector applications, IEEE Trans. Nucl. Sci. 51 (5 I) (2004) 2443–2447.
[26] NIST ASTAR, 2018, https://physics.nist.gov/PhysRefData/Star/Text/ASTAR.html, Access date: October 2018.
[27] NIST, 2017. http://physics.nist.gov/PhysRefData/Star/Text/ASTAR.html. Accesed July 2017.